UDK 620.1:537.226.86:621.77
Original scientific article/Izvirni znanstveni članek

ISSN 1580-2949
MTAEC9, 55(2)163(2021)

EXPERIMENTAL INVESTIGATION ON STRESS AND DIE-WALL FRICTIONAL CHARACTERISTICS OF METAL POWDER DURING HIGH-VELOCITY COMPACTION

EKSPERIMENTALNA RAZISKAVA NAPETOSTI IN ZNAČILNOSTI TRENJA NA STENAH ORODJA ZA STISKANJE KOVINSKIH PRAHOV Z VELIKO HITROSTJO

Wei Zhang[1*], Kun Liu[2], Jian Zhou[2], Rongxin Chen[2], Ning Zhang[1], Guofu Lian[1]

[1]School of Mechanical & Automotive Engineering, Fujian University of Technology, Fuzhou 350118, China
[2]Institute of Tribology, Hefei University of Technology, Hefei 230009, China

Prejem rokopisa – received: 2019-12-19; sprejem za objavo – accepted for publication: 2021-01-04

doi:10.17222/mit.2019.300

In this study, to evaluate the change in the stress and die-wall frictional characteristics during high-velocity compaction (HVC), a metal powder was subjected to HVC with a heavy hammer based on the stress-testing technology and Janssen-Walker model. The changes in the green density, stress characteristics and coefficients of friction at different impact heights were investigated. The density of green compacts increased with the increase in the impact height. The stress in the upper and lower punches and the die wall showed repeated loading and unloading. The coefficient of friction of the die wall underwent three stages and was related to powder densification. As the height position along the side wall was increased, the coefficient of friction increased gradually. With an increased impact height, the coefficient of friction increased significantly in the incomplete-molding stage but remained constant in the complete-molding stage. This work expands the theoretical basis of densification processing of a metal powder during HVC.

Keywords: metal powder, high-velocity compaction, friction coefficient , stress

V članku avtorji predstavljajo študijo napetostnih sprememb in značilnosti trenja na stenah orodja med stiskanjem (kompaktiranjem) kovinskega prahu z veliko hitrostjo. Kovinski prah so izpostavili stiskanju z veliko hitrostjo s pomočjo težkega kladiva na osnovi napetostno-preizkusne tehnologije in Janssen–Walkerjevega modela. Med preizkusi so ugotavljali spremembe v zeleni gostoti, napetostnih karakteristikah in koeficiente trenja pri različnih hitrostih udarcev kladiva. Zelena gostota je naraščala z naraščajočo hitrostjo udarcev. Sprememba napetosti v zgornjem in spodnjem trnu ter stenah orodja se je ujemala z izmeničnim obremenjevanjem in razbremenjevanjem. Koeficient trenja na stenah orodja je prestal tri različne stadije povezane z zgoščevanjem prahu. S povečevanjem stranske višine stene, se je postopno povečeval tudi koeficient trenja. S povečevanjem udarne višine se je tudi koeficient trenja pomembno povečeval v ne popolnoma oblikovanem stadiju, toda ostal je konstanten v stadiju popolnega oblikovanja (zgoščevanja). To delo, po mnenju avtorjev, razširja teoretična dognanja procesa zgoščevanja kovinskih prahov z veliko hitrostjo.

Ključne besede: kovinski prah, stiskanje z veliko hitrostjo, koeficient trenja, napetosti

1 INTRODUCTION

High velocity compaction (HVC) is a novel formation method in the powder-metallurgy industry. Essentially, HVC involves a rapid densification of a powder by applying a high-impact load at 2–30 m/s.[1] During HVC, the powder undergoes a quicker reorganization, rearrangement, and densification relative to the conventional compaction (CC). Hence, HVC is advantageous over the other formation technologies due to its high production efficiency, low spring back, high green density and good density uniformity.[2] HVC causes a higher density and better density uniformity than CC due to its stress wave.[3] And most of the research[2,3] captures axial stress to analyze the stress wave in HVC. A quick local arrangement and elastic-plastic deformation of a powder are present in HVC. However, the influence of the die-wall friction and rapid evolution of stress on densification need further investigation.

The frictional mechanism of a powder compaction has been extensively studied. F. Güner et al.[4] used the multi-particle finite-element method and experimentally studied the differences among friction models, such as Coulomb's and Levanov's models, and pointed out that different friction models are suitable for different pressure values and deformation characteristics of powders. S. Turenne et al.[5] investigated the influence of the admixed lubricant content on various coefficients of friction in powder compaction, wherein an increased stress ratio and appropriate admixed lubricant content lowered the slide coefficient. H. Staf et al.[6] proposed a method to calculate the local coefficient of friction in powder compaction and established a relationship between the normal pressure and coefficients of friction. Usually, friction is not good for the densification of a powder, and studies have been mostly concerned about the friction mecha-

*Corresponding author's e-mail:
zw1256@fjut.edu.cn (Wei Zhang)

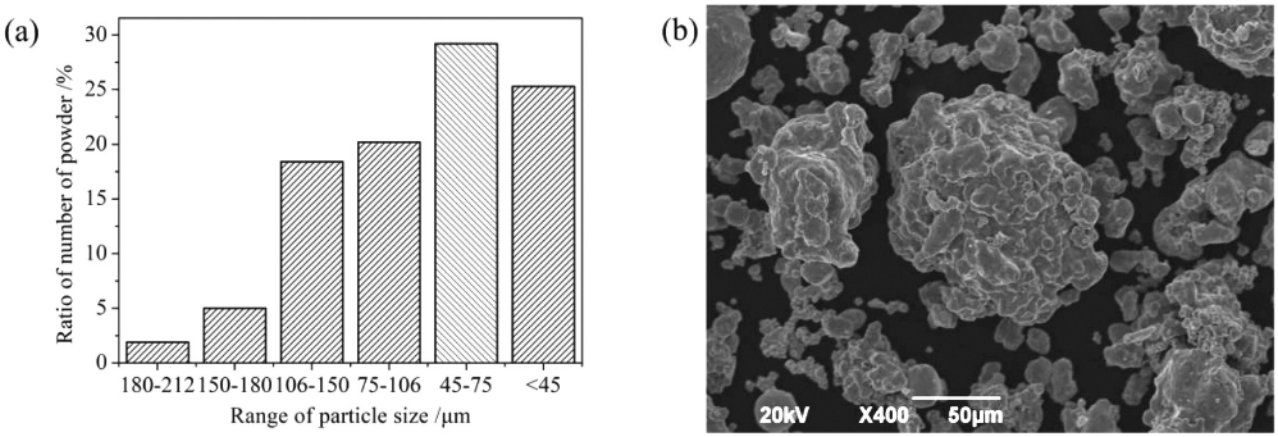

Figure 1: Powder information: a) particle size distribution and b) micromorphology of the powder

nism in CC. Compared with CC, stress increases quicker under a high-velocity impact load in HVC and frictional characteristics have a more significant influence on the densification and density uniformity of a powder.[7] The conditions of the relative slip and contact between a powder and die wall undergo a rapid evolution in HVC. Hence, the friction and stress characteristics in HVC may be more complex than in CC.

The current work experimentally determines the evolution of stress characteristics and die-wall coefficients of friction at different impact heights in the HVC of a Distaloy AE powder, based on the stress-testing technology and the Janssen-Walker model. This study aims to expand the theoretical basis of the densification and density homogenization of powders during HVC, based on stress and frictional characteristics.

2 EXPERIMENTAL PART

2.1 Materials and a HVC device

A Distaloy AE powder was supplied by Hefei Bolin Advance Materials Ltd., China. Its chemical composition is given in **Table 1**. Its apparent density and green density are 3.07 g/cm^3 and 7.16 g/cm^3, respectively. Its flowability is about 2 g/s. It has a mean diameter of 77 μm and the particle size distribution is shown in **Figure 1a**. The powder particles have an irregular, rounded shape and rough surfaces, as shown in **Figure 1b**. Microstructural observation was carried out on a JSM-6490LV-type SEM machine (JEOL Ltd., Tokyo, Japan).

Table 1: Chemical composition of Distaloy AE powder

Element	Fe	Ni	Cu	Mo	C
w/%	Balance	4.01	1.48	0.49	0.09

The independently developed BL-GSTZ-1-type HVC device (Bolin Advanced Materials Ltd., Hefei, China) was used to compress the Distaloy AE powder and utilize a drop hammer device. **Figure 2a** shows the structure of this device. The impact heavy hammer weighed 50 kg, and 24 g of powder filled a 16-mm-diameter cylindrical die. The impact height was set between 0.4–1.6 m with a 0.2 m interval.

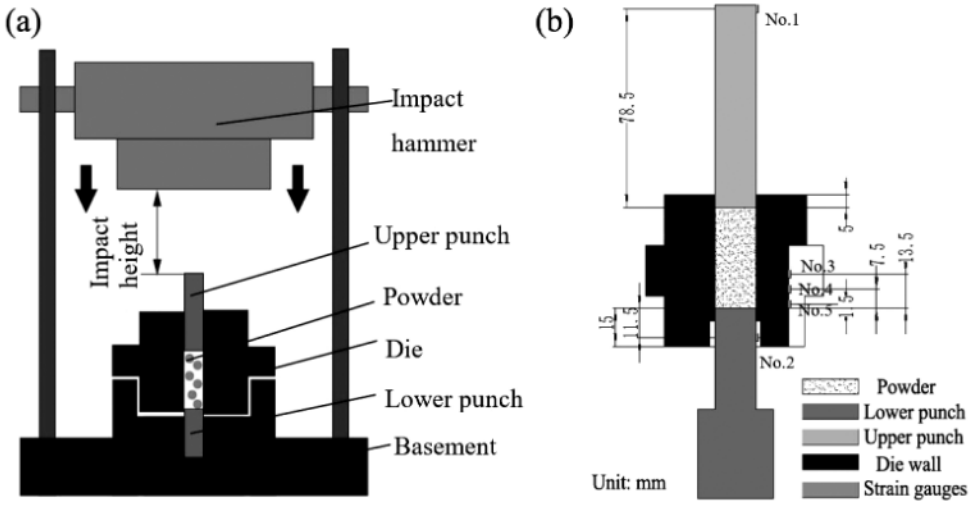

Figure 2: Schematic diagram of the HVC device: a) structure and b) adhesive positions of strain gauges

Five BX120-1AA-type strain gauges (Hope Technologic Ltd., Xiamen, China) were stuck at different positions on the die, as shown in **Figure 2b**. No. 1 and No. 2 were used to capture the strain of the upper and lower punches, respectively. No. 3 to No. 5 were used to capture the strains of the die wall. The distances from the center of No. 3 to No. 5 to the top surface of the bottom punch were 13.5, 7.5 and 1.5 mm, respectively. The strains were recorded with a SA-DYB0801-type dynamic strain indicator (Shiao Technology Ltd., Wuxi, China) and a computer.

2.2 Calibration of the stress-strain relation

To capture the stress, the relationship between stress and strain was calibrated using a BL-JX-SY-046-type universal material-testing machine (Bolin Advanced Materials Ltd., Hefei, China). Cylindrical silicon rubber with a diameter of slightly less than 16 mm and a height of 25 mm was used to fill in the die and was then compressed at a velocity of 5 mm/min. The axial and radial stresses were determined based on the incompressibility characteristic (Poisson's ratio was about 0.5) of the silicon rubber.[8] The strains of the gauges were recorded simultaneously. Thus, the relationship between the stress and strain of the upper and lower punches and the die wall can be determined as follows:

$$\sigma_{\text{top}} = 0.62\varepsilon_{\text{top}} \tag{1}$$

$$\sigma_{\text{bottom}} = 0.105\varepsilon_{\text{bottom}} \tag{2}$$

$$\sigma_{\text{wall}} = 0.74\varepsilon_{\text{wall}} \tag{3}$$

where σ_{top}, σ_{bottom} and σ_{wall} are the stresses and ε_{top}, $\varepsilon_{\text{bottom}}$ and $\varepsilon_{\text{wall}}$ are the strains of the upper punch, lower punch and the die wall, respectively.

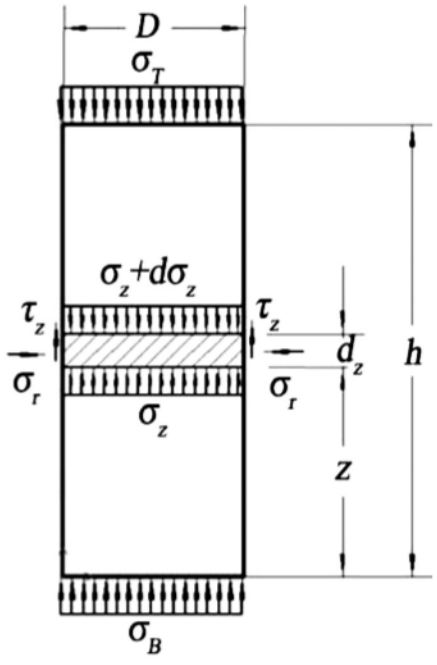

Figure 3: Force analysis of the powder

2.3 Determination of the die-wall coefficient of friction

HVC was completed within a short time and the direct measurement of the die-wall coefficient of friction was difficult to carry out. Hence, it was analyzed based on the Janssen-Walker model in HVC.[9] The two-dimensional cross-section of the cylindrical powder was analyzed, as shown in **Figure 3**. By assuming uniform vertical stresses along the horizontal cross-sections, arbitrary elemental slices with a thickness of d_z at a distance of z from the bottom of the powder were considered based on the force equilibrium, as follows:

$$\frac{\pi D^2}{4}\mathrm{d}\sigma_z + \rho\frac{\pi D^2\mathrm{d}z}{4}g = \tau_z \pi D\mathrm{d}z \tag{4}$$

where σ_z and τ_z are the axial and radial stresses, respectively, at a height of z, D is the diameter of the cylindrical powder, and ρ and g are the densities and gravitational acceleration, respectively.

The d_z values were small, rendering the masses of slices negligible. Combined with Coulomb's law and the lateral-pressure coefficient, Equation (4) can be transformed as follows:

$$\frac{\mathrm{d}\sigma_z}{\sigma_z} = \frac{4k\mu}{D}\mathrm{d}z \tag{5}$$

where k is the lateral-pressure coefficient and μ is the coefficient of friction.

Considering the relative boundary condition, Equation (5) can be integrated as follows:

$$\sigma_z = \sigma_{\text{B}}\left(\frac{\sigma_{\text{T}}}{\sigma_{\text{B}}}\right)^{z/h} \tag{6}$$

From Equations (5) and (6), the coefficient of friction μ can be calculated as follows:

$$\mu = \frac{D}{4h}\frac{\sigma_{\text{B}}}{\sigma_{\text{r}}}\left(\frac{\sigma_{\text{T}}}{\sigma_{\text{B}}}\right)^{z/h}\ln\left(\frac{\sigma_{\text{T}}}{\sigma_{\text{B}}}\right) \tag{7}$$

where σ_{T}, σ_{B} and σ_{r} are the stresses in the upper punch, lower punch and die wall, respectively. The determination of the coefficient of friction is detailed in [10].

3 RESULTS AND DISCUSSION

3.1 Green-density analysis

In this study, the Distaloy AE powder was compressed at impact heights of 0.4–1.6 m with a 0.2 m interval. The green compacts obtained at an impact height of 0.4–1 m exhibited the phenomenon of stratification. Hence, we defined these impact heights as incomplete-molding impact heights (0.4, 0.6, 0.8 and 1) m. The green compacts obtained at an impact height of 1.2–1.6 m did not exhibit visible stratification. Hence, we defined these impact heights as complete-molding impact heights (1.2, 1.4 and 1.6) m.

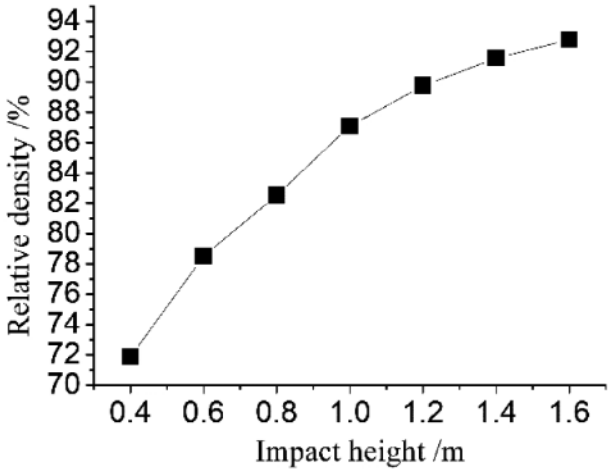

Figure 4: Variation in the green density at different impact heights

According to the geometric measurement of density, the relative density increased with the increase in the impact height, as shown in **Figure 4**. At incomplete-molding impact heights, the relative density rapidly increased from 71.9 % to 87.1 %, whereas the growth rate became slow (from 89.7 % to 92.8 %) at complete-molding impact heights. The figure shows a linear increase at the incomplete-molding stage, and a non-linear (logarithmic) increase at the complete-molding stage. This may be attributed to the molding state of the powder. A detail discussion of this phenomenon will be carried out in the future.

3.2 Stress-characteristics analysis

The increase in the relative density is small when the impact height changes from 1.2 m to 1.6 m at the complete-molding stage. Thus, the middle impact height of 1.4 m was selected to be analyzed. **Figure 5a** shows the time evolution of stress at an impact height of 1.4 m, with several stress peaks during HVC. Every peak consists of the loading and unloading stages under impact loading. Moreover, the peak values show a decay tendency due to the loss of impact energy. Wang et al.[1] stated that the compact pressure is dominant at the first peak, which has the highest influence on the densification in HVC. Hence, we only considered the stress and frictional characteristics at the first peak. The first peak from **Figure 5a** was amplified, as shown in **Figures 5b** and **5c**. The radial stresses decreased as the height position along the side wall increased, as shown in **Figure 5b**. The radial stress initially increased and then decreased. The middle and lower parts showed a higher stress than the upper part. Furthermore, the stress on the

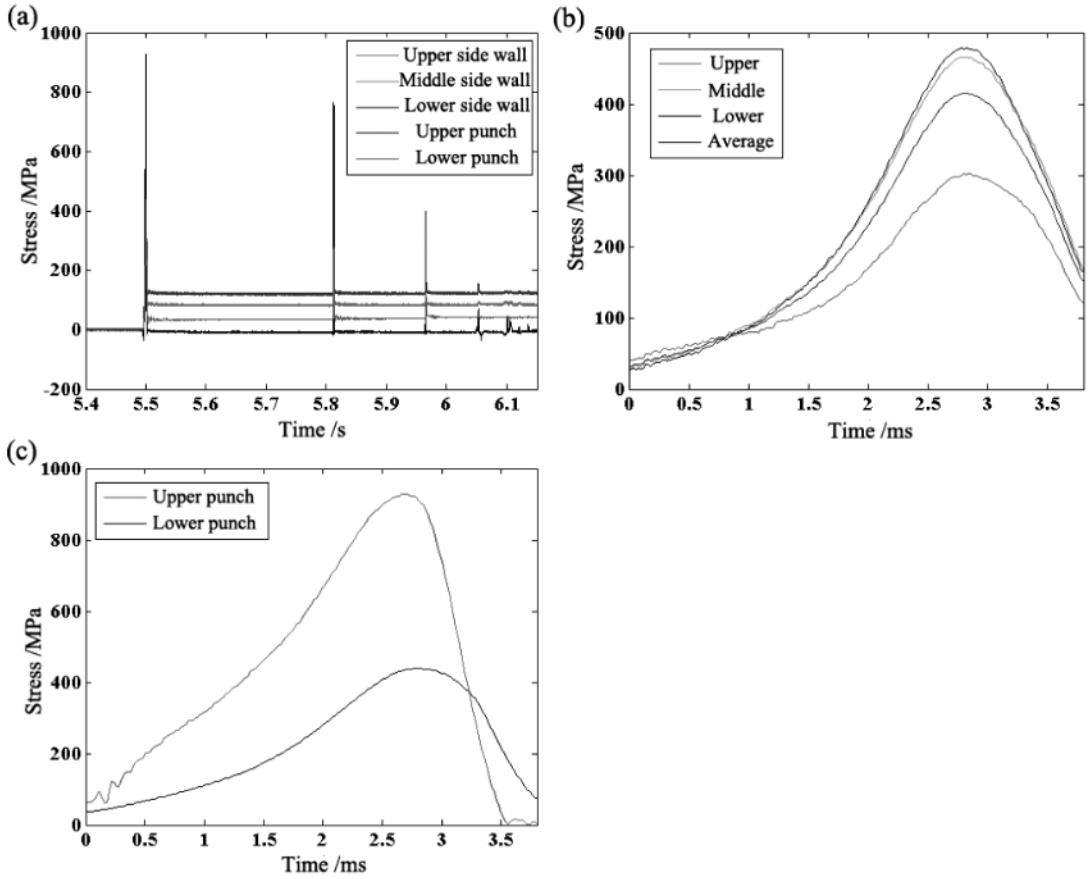

Figure 5: Variation in the stress at the impact height of 1.4 m: a) total stress peaks, b) radial stresses at the first stress peak, and c) axial stresses at the first stress peak

upper and lower punch initially increased and then decreased, as shown in **Figure 5c**. The upper punch stress was greater than the lower punch stress, consisting of the loading (0–2.8 ms) and unloading (2.8–3.5 ms) stages.

The influence of the impact heights on the stress characteristics was investigated. **Figure 6a** shows the maximum axial-stress increase as the impact height increases. The maximum axial stresses increased from 300 MPa to 500 MPa at the incomplete-molding impact heights, and from 600 MPa to 1150 MPa at the complete-molding impact heights. Moreover, the maximum axial stresses at the complete-molding impact heights showed a wider change range than at the incomplete-molding impact heights. A high green density could be achieved under a high compaction stress and the increase in the green density at the complete-molding impact heights needed a higher compaction stress. **Figure 6b** shows the maximum radial-stress increase as the impact height increases, too. When comparing **Figures 6a** and **6b**, we can say that although the maximum axial stress is higher than the maximum radial stress, they have a similar change tendency. They increased slowly at the incomplete-molding impact heights and then increased quickly at the complete-molding impact heights.

The loading, unloading and duration times decreased as the impact heights increased, as shown in **Figure 6c**. The duration time refers to the time consumed up to the first peak, which consists of the loading and unloading times. At the complete-molding impact heights, the duration and loading time decreased, but the unloading time was maintained at about 1 ms. Wang et al.[11] and Zhang et al.[12] found that the duration time decreases as the impact energy increases, and this finding is consistent with our results, but we further discuss the loading and unloading times.

The proportion of the loading time at the complete-molding impact heights is higher than at the incomplete-molding impact heights, as shown in **Figure 6d**. The proportion refers to the ratio of the loading time to duration time. The proportion of the loading time at the incomplete-molding impact heights was maintained at about 64 %. Conversely, the proportion of the loading time decreased at the complete-molding impact heights as the impact heights increased and it was higher than 64 %.

3.3 Coefficient-of-friction analysis

The time evolution for the coefficients of friction at the first peak at the complete-molding impact heights is shown in **Figure 7**.

The coefficients of friction decreased with the decrease in the height position along the side wall, as shown in **Figure 7**. Relative-slip velocities between the

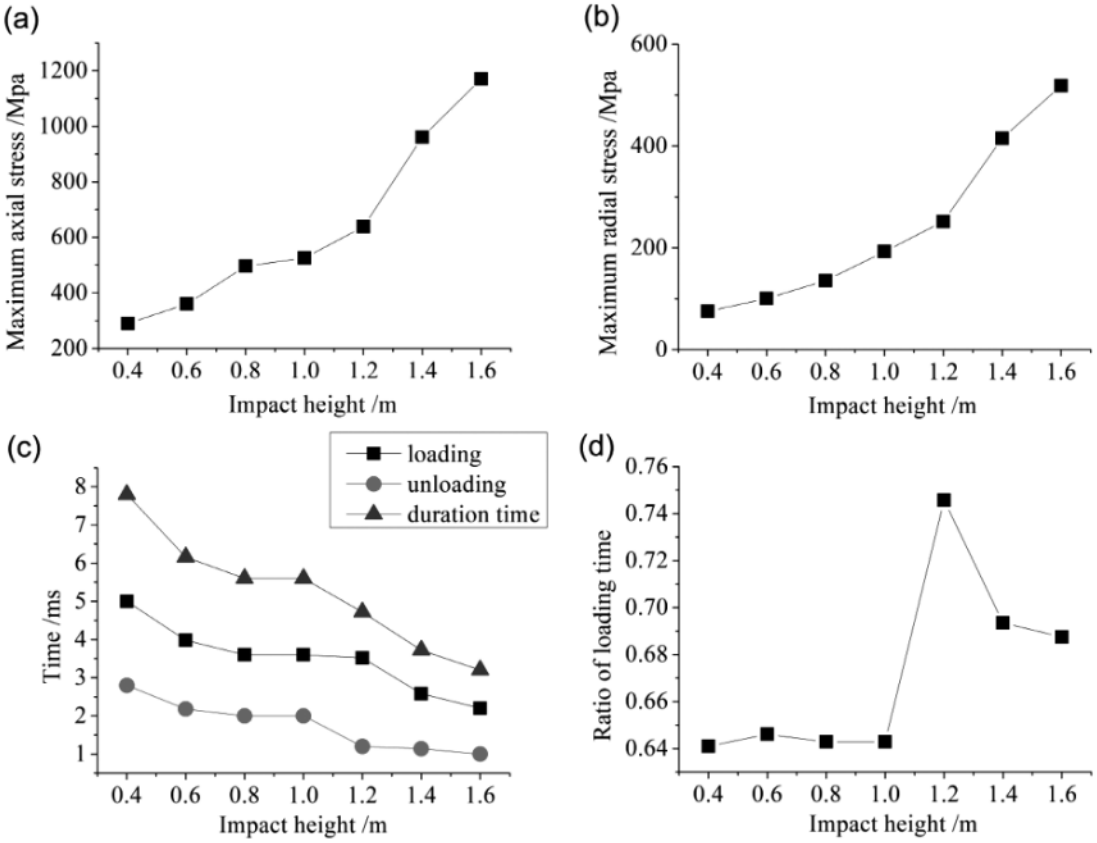

Figure 6: Stress characteristics at different impact heights: a) maximum axial stresses, b) maximum radial stresses, c) characteristic time of the stress, d) proportion of the loading time

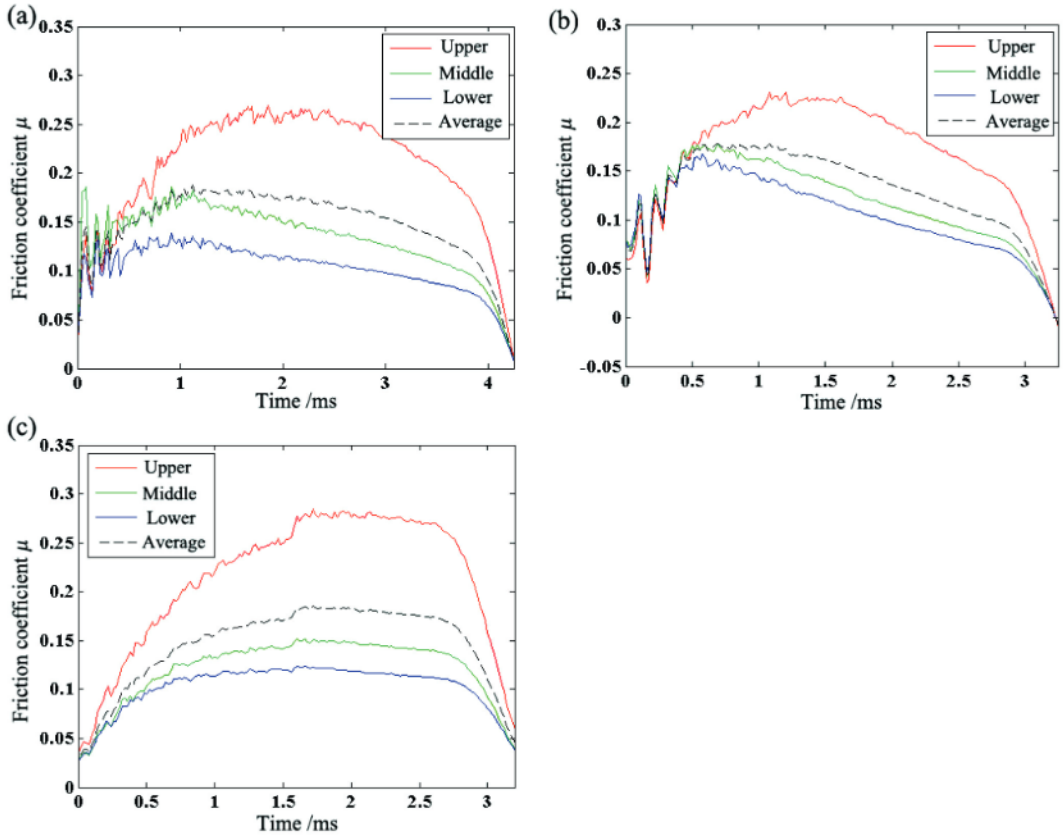

Figure 7: Variation of coefficients of friction at the impact heights of: a) 1.2 m, b) 1.4 m, c) 1.6 m

powder and die wall at different height positions along the side wall during HVC exhibited small differences. The load was essential for the changes in the coefficients of friction. The radial stress increased with the decrease in the height position along the side wall. According to the friction adhesion theory,[13] the contact area between the powder and sidewall increases with a load increase. The contact interfaces become smoother and the meshing of the rough peak between the powder and die wall decreases gradually under elastic-plastic contact conditions.[14] Thus, the coefficients of friction decrease as the height position decreases.

The coefficients of friction initially increase, then remain stable or slightly decrease and finally decrease significantly at different impact heights. For example, the change in the coefficients of friction with the time at an impact height of 1.4 m is shown in **Figure 7b**. During loading (0–2.8 ms), a relative slip occurs between the powder and die wall. Hence, the coefficient of friction initially fluctuates with an upward trend (0–0.5 ms). Afterward, the stick and slip between the powder and die wall occur constantly with the deformation of the powder and the relative slip between the powder and die wall. The coefficients of friction remain stable during a decreasing trend (0.5–2.8 ms), with an increase in the slip velocity and change in the stick time amplitude. [13] During unloading (2.8–3.5 ms), the relative slip gradually stops, and the coefficients of friction decrease significantly. Combined with the powder-densification process in HVC, the relationship between the normal pressure of the die wall and the coefficients of friction at an impact height of 1.4 m is shown in **Figure 8**.

Initial stage I (0–80 MPa) of HVC is dominated by powder displacement and rearrangement. The number of contact points between the powder and die wall increase with the increase in the normal pressure. Hence, the flow

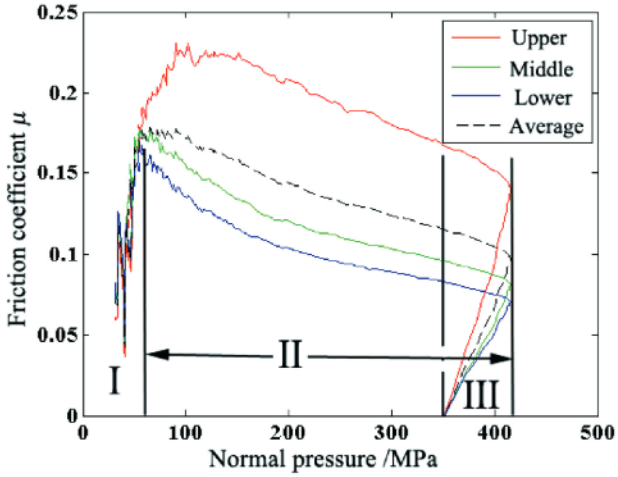

Figure 8: Relationship between the normal pressure and coefficient of friction

capacity of the powder decreases and the contact condition changes frequently. The coefficients of friction fluctuate with an upward trend. Stage II (80–410 MPa) of HVC is dominated by elastic and plastic deformations of the powder. A uniform porous densification of powder is gradually formed at a high stress. The flow capacity of the powder stabilizes and the contact interface smoothens. Hence, the coefficients of friction are maintained at about 0.1–0.2, which is close to the standard value for metals. [6] Stage III (410–350 MPa) of HVC is dominated by unloading with springback. The normal pressure decreases and the contact area between the powder and die wall also decreases in accordance with the elastic recovery of the powder. The adhesive force becomes weak. Hence, the coefficients of friction decrease significantly.

Figure 9 shows that the coefficients of friction initially increase, then decrease significantly and finally increase slightly with the increase in the impact height. A remarkable decrease in the friction coefficient occurs when the formation behavior changes (0.8–1 m). During incomplete molding (0.4–1 m), the powder system transforms from loose to dense, and the flow capacity decreases. Hence, the coefficients of friction increase. During complete molding (1.2–1.6 m), the coefficients of friction are maintained at about 0.175. The coefficient of friction during common compaction of iron powder ranges from 0.15 to 0.2.[5] Thus, the coefficients of friction in our analysis are reasonable. An increase in the load can reduce the coefficients of friction, whereas an increase in the relative slip velocities can increase the coefficients of friction.[13] Hence, coefficients of friction slightly change under the mutual effects of the load and relative slip velocities. Furthermore, the coefficients of friction are close to the original values after a small increase in the green density but exhibit a remarkable increase with a significant increase in the green density. The densification of a powder can affect the coefficients of friction to some extent.

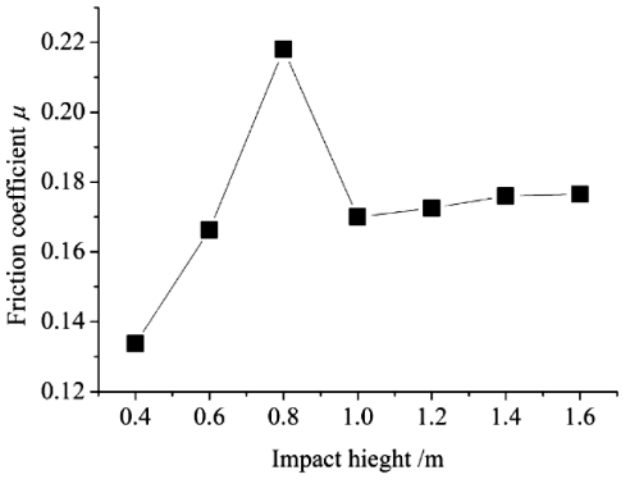

Figure 9: Variation of coefficients of friction at different impact heights

4 CONCLUSIONS

The following conclusions can be drawn:

1) The relative density increases with the increased impact height and exhibits different variations at incomplete- and complete-molding impact heights.

2) The time evolution of stress has several loading-unloading stages in HVC with a decrease in the maximum peak stresses. The maximum axial stress increases with the increased impact height. The loading, unloading and duration times decrease with the increased impact height. The proportion of the loading time remains constant during the incomplete-molding stage, whereas it decreases with the increased impact height during the complete-molding stage. The radial stresses increase with the decrease in the height position along the side wall.

3) The coefficients of friction of the die wall initially increase, then remain stable, or slightly decrease, and finally decrease significantly. This is related to the normal pressure of the die wall. The coefficients of friction gradually increase with the increase in the height position along the side wall. Furthermore, the coefficients of friction significantly increase with the increase in the impact heights during the incomplete-molding stage but remain constant (0.175) during the complete-molding stage.

Acknowledgment

This research was funded by the National Natural Science Foundation of China (No. 51975174), the Natural Science Foundation of the Fujian Province (Grant No. 2020J01869) and the Initial Scientific Research Fund from the Fujian University of Technology (Grant No. GY-Z19123). The authors gratefully acknowledge the support from the Public Service Platform for Technical Innovation of Machine Tool Industry at the Fujian University of Technology in the Fujian Province.

5 REFERENCES

[1] J. Z. Wang, X. H. Qu, H. Q. Yin, M. J. Yi, X. J. Yuan, High velocity compaction of ferrous powder, Powder. Technol., 192 (**2009**) 1, 131–136, doi:10.1016/j.powtec.2008.12.007

[2] H. Li, H. Q. Yin, D. F. Khan, H. Q. Cao, Z. Abideen, X. H. Qu, High velocity compaction of $0.9Al_2O_3$/Cu composite powder, Mater. Design., 57 (**2014**), 546–550, doi:10.1016/j.matdes.2013.12.059

[3] B. Azhdar, B. Stenberg, L. Kari, Development of a high-velocity compaction process for polymer powders, Polym. Test., 24 (**2005**) 7, 909–919, doi:10.1016/j.polymertesting.2005.06.008

[4] F. Güner, Ö. N. Cora, H. Sofuoğlu, Effects of friction models on the compaction behavior of copper powder, Tribol. Int., 122 (**2018**), 125–132, doi:10.1016/j.triboint.2018.02.022

[5] S. Turenne, C. Godère, Y. Thomas, P.-É. Mongeon, Evaluation of friction conditions in powder compaction for admixed and die wall lubrication, Powder Metall., 42 (**1999**) 3, 263–268, doi:10.1179/003258999665611

[6] H. Staf, E. Olsson, P. Lindskog, P. L. Larsson, Determination of the frictional behavior at compaction of powder materials consisting of

spray-dried granules, J. Mater. Eng. Perform., 27 (**2018**) 3, 1308–1317, doi:10.1007/s11665-018-3205-1

[7] B. J. Briscoe, S. L. Rough, The effects of wall friction in powder compaction, Colloid. Surfaces A, 137 (**1998**) 1, 103–116, doi:10.1016/S0927-7757(97)00210-0

[8] E. Doelker, D. Massuelle, Benefits of die-wall instrumentation for research and development in tableting, Eur. J. Pharm. Biopharm., 58 (**2004**) 2, 427–444, doi:10.1016/j.ejpb.2004.03.011

[9] R. M. Nedderman, Statics and kinematics of granular materials, Cambridge University Press, Cambridge 1992

[10] C.-Y. Wu, O. M. Ruddy, A. C. Bentham, B. C. Hancock, S. M. Best, J. A. Elliott, Modelling the mechanical behavior of pharmaceutical powders during compaction, Powder Technol., 152 (**2005**) 1, 107–117, doi:10.1016/j.powtec.2005.01.010

[11] J. Z. Wang, H. Q. Yin, X. H. Qu, J. L. Johnson, Effect of multiple impacts on high velocity pressed iron powder, Powder Technol., 195 (**2009**) 3, 184–189, doi:10.1016/j.powtec.2009.05.028

[12] H. Z. Zhang, L. Zhang, G. Q. Dong, Z. W. Liu, M. L. Qin, X. H. Qu, Y. Z. Lü, Effects of annealing on high velocity compaction behavior and mechanical properties of iron-base PM alloy, Powder Technol., 288 (**2016**), 435–440, doi:10.1016/j.powtec.2015.10.040

[13] F. P. Bowden, D. Tabor, The Friction and Lubrication of Solids, Oxford University Press, Oxford 1954

[14] J. P. Gao, W. D. Luedtke, D. Gourdon, M. Ruths, J. N. Israelachvili, U. Landman, Frictional forces and Amontons' law: from the molecular to the macroscopic scale, J. Phys. Chem. B., 108 (**2004**) 11, 3410–3425, doi:10.1021/jp036362l